Combined Assessment of Beat-to-Beat Micro-variability and Signal-averaged ECG Parameters

HA Kestler[1,2], F Schwenker[1], J Wöhrle[2], V Hombach[2], G Palm[1], M Höher[2]

[1]Neural Information Processing, University of Ulm, Germany
[2]Medicine II – Cardiology, University Hospital Ulm, Germany

Abstract

Increased QRS- and ST-T micro-variability and ventricular late potentials are associated with an increased risk for malignant arrhythmias. However, the diagnostic power of the singular parameters is limited. In this study we investigated the diagnostic ability of a linear combination of both variant and static high-resolution ECG parameters. Continuous and signal-averaged ECGs were recorded from 51 healthy volunteers without any structural heart disease and no cardiac risk factors and from 44 patients with coronary heart disease and ventricular arrhythmias. Beat-to-beat micro-variability measurement of the QRS complex and the ST-T segment was based on 250 consecutive sinus beats per individual. Signal-averaged ECGs were analyzed with the Simson method (QRSD, RMS, LAS). The diagnostic utility of the 5 singular parameters and all combinations of variables were evaluated by linear discriminant analysis maximizing the area under the receiver operator characteristic curve. We conclude that the combination of de- and repolarization variability with the static QRS duration markedly improves the detection of patients with inducible VT.

1. Background

High-resolution electrocardiography is used for the detection of fractionated micropotentials, which serve as a non-invasive marker for an arrhythmogenic substrate and for an increased risk for malignant ventricular tachyarrhythmias. Beat–to–beat variation of cardiac excitation and depolarization has been associated with electrical instability and an increased risk for arrhythmias [1]. Rosenbaum et al. [2] have shown that increased beat–to–beat microvariations of the T–wave, although visually inapparent, are associated with a decreased arrhythmia–free survival. Their method to quantify periodic electrical alternans of the T–wave amplitude has gained growing clinical acceptance as a non–invasive, electrocardiographic risk marker. Earlier high–resolution electrocardiographic studies already demonstrated periodic and non-periodic behaviour of ventricular late potentials at the terminal QRS [3–6]. Previous work of our group showed a significantly higher beat–to–beat variation of the duration of the filtered QRS [7] and an increased total beat–to–beat microvolt variation of both the QRS and the ST-T segment [8] among patients with an increased risk for ventricular tachycardias.

The aim of this study was to utilize and evaluate markers of intra–QRS and ST-T beat–to–beat signal variation together with long known markers of the signal-averaged high-reolution ECG.

2. Subject data

We compared a group of 51 healthy subjects (group A) with 44 cardiac patients at a high risk for malignant ventricular arrhythmias (group B, VT patients). All healthy volunteers (mean age 24.0±4.1years) had a normal resting ECG and a normal echocardiogram, and no cardiac symptoms or coronary risk factors. The patients with a high–risk for malignant ventricular arrhythmias (mean age 61.2±8.9 years) were selected from our electrophysiologic database. Inclusion criteria were the presence of coronary artery disease, a previous myocardial infarction, a history of at least one symptomatic arrhythmia, and inducible sustained ventricular tachycardia (> 30 seconds) at electrophysiologic testing. Patients with bundle branch block or atrial fibrillation were excluded. All patients of group B underwent coronary angiography and programmed right ventricular stimulation due to clinical indications. Stimulation was done from the right apex and the right outflow tract. The stimulation protocol included up to 3 extrastimuli during sinus rhythm and at baseline pacing with a cycle length of 500ms, and a maximum of 2 extrastimuli at baseline pacing with cycle lengths of 430ms, 370ms, and 330ms. Group B consisted of 10 patients with single vessel disease, 17 patients with double vessel disease, and 17 patients with triple vessel coronary artery disease. Nineteen patients had a previous posterior infarction, 14 patients had a previous anterior infarction, and 11 patients had both a previous

0276-6547/01 $17.00 © 2001 IEEE

Computers in Cardiology 2001;28:73-76.

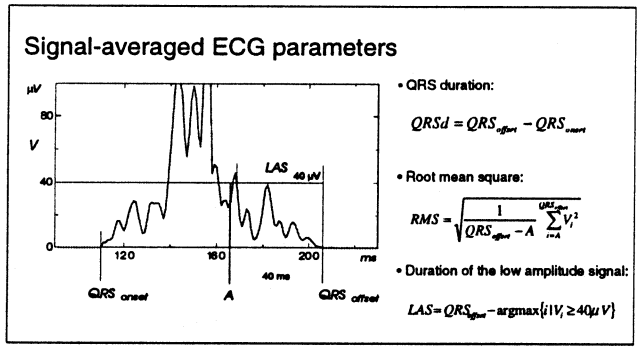

Figure 1. Parameters from the signal-averaged high-resolution ECG: Duration of the QRS complex (QRSd), and amplitude (RMS) and duration (LAS) of the terminal portion of the QRS which are used for ventricular late potential analysis.

anterior and a previous posterior infarction. Mean left ventricular ejection fraction was 44.0%±14.9%. Forty-one patients had a documented episode of spontaneous, sustained ventricular tachycardia or ventricular fibrillation. Out of the remaining three patients, 1 patient had syncopes and non–sustained ventricular tachycardias on Holter monitoring, and 2 patients had syncopes of presumed cardiac origin.

3. ECG recordings

High–resolution electrocardiograms were recorded during sinus rhythm from bipolar orthogonal X, Y, Z leads using the Predictor system (Corasonix Inc., Oklahoma, USA). A/D resolution was 16 bit with an antialiasing filter (0.05-300Hz). Before ECG recording antiarrhythmic drugs were stopped for at least four half–lives. The skin was carefully prepared and recordings were done with the subjects in reclining position in a Faraday cage. For signal-averaged recordings the sampling rate was 2000Hz. The three leads were combined into a vectormangnitude signal $V = \sqrt{X^2 + Y^2 + Z^2}$ and bidirectionally filtered with a 4 pole Butterworth filter (40-250Hz), see Figure 1. From this signal the three features of ventricular late potential analysis, QRS duration (QRSd), and the duration (LAS) and amplitude (RMS) of the terminal portion of the QRS complex were extracted. For the beat–to–beat recordings of 30min duration the sampling rate was reduced to 1000Hz. QRS triggering, reviewing of the ECG, and arrhythmia detection was done on a high–resolution ECG analysis platform developed by our group [9]. The three leads were summed into a signal $V = X + Y + Z$. From each recording 250 consecutive sinus beats preceded by another sinus beat were selected for subsequent beat–to–beat variability analysis. In a first step the signals were aligned by maximizing the cross–correlation function [10] between the first and all following beats. Prior to

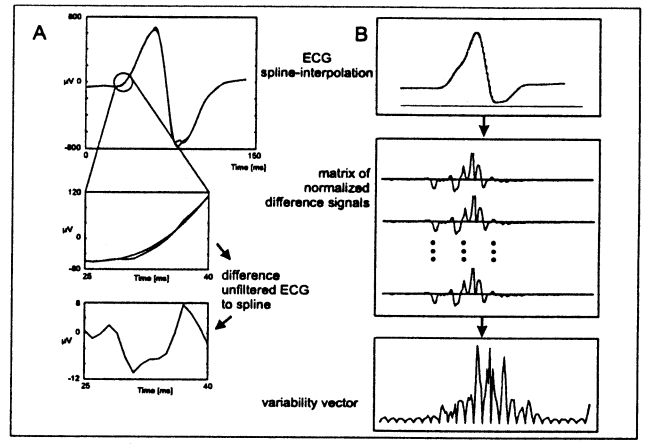

Figure 2. Diagram of the spline–filtering procedure. The upper left panel (A) shows both signals, the QRS–complex (sum of the three leads) and the cubic spline. A zoom–in makes the differences more apparent. The right panel (B) shows the calculation of the variability vector which is then summed into a variability index (QVI and TVI).

the quantification of signal variability the beats were pre-processed to suppress the main ECG waveform, bringing the beat–to–beat micro-variations into clearer focus. To achieve this, the individual signal was subtracted from its cubic spline smoothed version (spline filtering, spline interpolation through every seventh sample using the not–a–knot end condition) [11], compare Figure 2 panel (A). This method resembles a waveform adaptive, high–pass filtering without inducing phase–shift related artefacts. Next, for each individual beat the amplitude of the difference signal was normalized to zero mean and a standard deviation of 1μV, see Figure 2 panel B. Beat–to–beat variation of each point was measured as the standard deviation of the amplitude of corresponding points across all 250 beats. For the QRS we used a constant analysis window of 141 ms which covered all QRS complexes of this series [8]. The intra-QRS signal variability index (QVI) was defined as the sum of the standard deviations of corresponding points. Repolarization microvariability inside the ST-T segment (TVI) was measured with the same adaptive spline filtering technique (constant window starting at the QRS-offset of 400ms) but using 3 instead of 21 knots.

4. ROC curves

Receiver operator characteristic (ROC) curves are recommended to assess the diagnostic value of tests depending on a single cut–off value of a continuous variable. Historically, they were developed in engineering as a way to examine how well radar was able to distinguish signal from noise. ROC curves show the sensitivity (true–

positive rate) against the 1-specificity (false–positive rate) [12, 13], defined as follows. Suppose that p diagnostic markers are used on a control group (negative disease condition) of m subjects and a disease group of n patients with outcomes X_i $(i = 1, \ldots, m)$, and Y_j $(j = 1, \ldots, n)$. We assume that the X's and Y's are iid samples from two different distributions with cumulative distribution functions $F(x)$ and $G(y)$. The diagnostic test associated with a marker is called positive if the marker exceeds a given cut–off value of c. Sensitivity and specificity are then defined by $F(c)$ and $1 - G(c)$, respectively. The ROC curve is generated by $F(c), 1 - G(c)$ as c takes on all possible values. The most commonly used quantitative global index summarizing the information provided by the ROC curve is the area below the curve [14]. Bamber [15] noted that the area under this curve is equal to $P(Y > X)$. A large area indicates a good dicriminative ability of the marker with a single cut–off value. Su and Liu [16] have shown that Fisher's linear discriminant maximizes sensitivity uniformly over the entire range of specificity when the two distributions are assumed normal with proportional covariance matrices. We denote μ_x and μ_y as the sample mean vectors, and S_x and S_y as the covariance matrices. Under the stated normality conditions and the assumption of equal variances, i.e. the scaling factor between the matrices is 1, the linear transformation of the normally distributed vectors X and Y into $U = a^T X$ and $V = a^T Y$ with $a = ((S_x + S_y)/(m + n - 2))^{-1}(\mu_y - \mu_x)/2$ provides the largest area under the ROC curve. By this linear combination a new virtual diagnostic marker Z is generated [17, 18]. Using this new marker and defining R_i $(i = 1, \ldots, m)$ as the vector of the ranks of the values of Z for the controls and S_j $(j = 1, \ldots, n)$ for the patients obtained by ranking all $m + n$ values of Z. Then, as Mee [19] showed, is a non-parametric estimate for the area under the ROC curve obtained by: $\hat{A} = \sum_{j=1}^{n}(S_j - j)/mn$. An approximate $1 - 2\alpha$ confidence interval is given by $\{\hat{A} + .5C \pm \sqrt{C}[\hat{A}(1-\hat{A}) + .25C]^{1/2}\}/(1+C)$, with $C = Z^2_{1-\alpha/2}/\hat{N}$, and $\hat{N} = (\hat{A} - \hat{A}^2)/V$, and $V = (\sum_{i=1}^{m}(R_i - i)^2/mn^2 - (1 - \hat{A})^2)/(m - 1) + (\sum_{j=1}^{m}(S_j - j)^2/nm^2 - \hat{A}^2)/(n - 1)$. Z_α is the $1 - \alpha$ quantile for a standard normal distribution.

5. Results

The results of the empirical non-parametric estimates of all 31 marker combinations are given in Figure 3. The singular parameters differ greatly in their area under the ROC curve: QRSd=.874, RMS=.784, LAS=.762, QVI=.753, TVI=.811. Among these QRSd was the most discriminative single variable. Combining both variability markers resulted in an area of QVI&TVI=.852. The combination of QRS duration with either QRS- or ST-T variability was both highly discriminative QRSd&QVI=.915 and QRSd&TVI=.898. The combination of QRSd, QVI and TVI yielded the highest area with the lowest number of parameters of .934. Including either RMS or LAS, or both did not increase the area. The ROC curve for the best linear combination is shown in Figure 4. The classification details are given in Table 1.

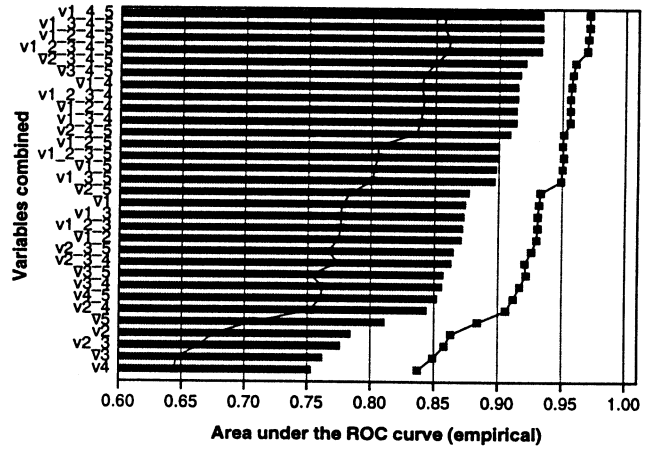

Figure 3. Ranking of marker combinations using the maximal area under the ROC curve (bar graph and 95% confidence intervals). Markers: v1=QRSd,v2=RMS, v3=LAS, v4=QVI, v5=TVI.

Table 1. **Classification results for the model of Figure 4** Acc: accuracy, Sensi: sensitivity, Speci: specificity, PPV: positive predictive value, NPV: negative predictive value, Re-val: training and test on the same data, Cross-val: 10-fold cross-validation (mean ± stdv, 1000 repetitions)

%	Acc	Sensi	Speci
Re-val	89.5	86.4	92.2
Cross-val	87.3±0.61	86.3±0.44	88.1±1.09
		PPV	NPV
Re-val		90.5	88.7
Cross-val		86.3±1.08	88.2±0.38

6. Conclusion

Ranking of the different marker combinations, although computationally intensive, gives valuable insights into the relevance of the diagnostic parameters. Most noticeably is the apparent lack of valuable information provided by RMS and LAS. Despite the difference of the subject groups a remarkable sensitivity of 86.4% and specificity of 92.2% (10 fold cross-validation: sensitivity=86.3% and specificity=88.1%) were attainable with the simple linear model consisting of QRSd, QVI and TVI. We conclude that the combination of de- and repolarization variability with the static QRS duration markedly improves

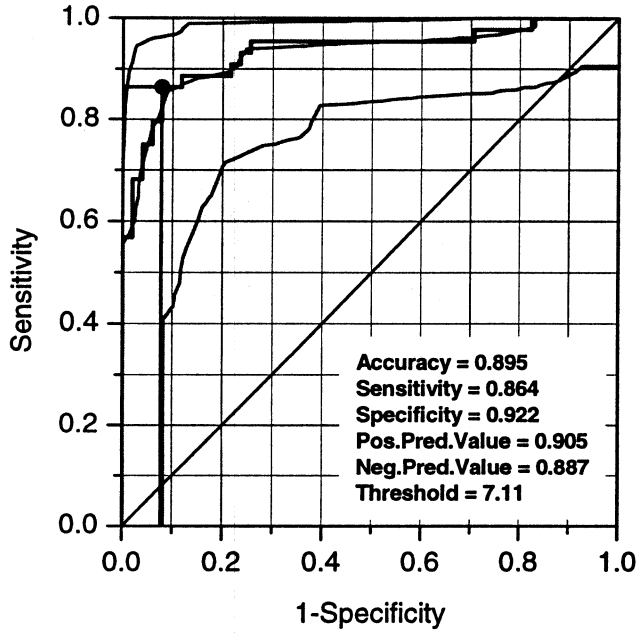

$$Z = 0.042 \times QRSd + 0.051 \times QVI + 0.022 \times TVI$$

Area under the ROC curve: 0.934
95% confidence interval: [0.858; 0.971]

Figure 4. Diagram of the ROC curve with its 95% confidence curves of the best linear combination (see Figure 3) of markers. Both the estimated (smooth) and the empirical ROC curve are displayed. The values denote the discriminative ability of the "diagnostic test" at the cut-off point (threshold) maximizing sensitivity and specificity.

the detection of patients with inducible VT. The use of linear discriminant analysis together with ROC provides a powerful yet simple tool to evaluate the diagnostic ability of multivariate data sets.

References

[1] Smith J, Clancy E, Valeri C, Ruskin J, Cohen R. Electrical alternans and cardiac electrical instability. Circulation 1988;77(1):110–121.

[2] Rosenbaum D, Jackson L, Smith J, Garan H, Ruskin J, Cohen R. Electrical Alternans and Vulnerability to Ventricular Arrhythmias. N Engl J Med 1994;330(4):235–41.

[3] Hombach V, Kebbel U, Höpp HW, Winter U, Hirche H. Noninvasive beat-by-beat registration of ventricular late potentials using high resolution electrocardiography. Int J Cardiol 1984;6:167–183.

[4] Hombach V, Kochs M, Höpp HW, et al. Dynamic behavior of ventricular late potentials. In Hombach V, Hilger HH, Kennedy HL (eds.), Electrocardiography and cardiac drug therapy. Dordrecht, Netherlands: Kluwer Academic Publishers, 1989; 218–238.

[5] Sherif NE, Gomes J, Restivo M, Mehra R. Late potentials and arrhythmogenesis. Pacing Clin Electrophysiol 1985; 8:440.

[6] Sherif NE, Gough W, Restivo M, Craelius W, Henkin R, Caref E. Electrophysiological basis of ventricular late potentials. Pacing Clin Electrophysiol 1990;13:2140–7.

[7] Höher M, Axmann J, Eggeling T, Kochs M, Weismüller P, Hombach V. Beat-to-beat variability of ventricular late potentials in the unaveraged high resolution electrocardiogram - effects of antiarrhythmic drugs. Eur Heart J 1993;14:E:33–39.

[8] Kestler HA, Wöhrle J, Höher M. Cardiac vulnerability assessment from electrical microvariability of the high-resolution electrocardiogram. Medical Biological Engineering Computing 2000;38:88–92.

[9] Ritscher DE, Ernst E, Kammrath HG, Hombach V, Höher M. High–Resolution ECG Analysis Platform with Enhanced Resolution. Computers in Cardiology 1997; 24:291–294.

[10] van Bemmel J, Musen M (eds.). Handbook of Medical Informatics. Heidelberg / New York: Springer Verlag, 1997.

[11] de Boor C. A Practical Guide to Splines. Springer Verlag, 1978.

[12] Lang T, Secic M. How to Report Statistics in Medicine. American College of Physicians, 1997.

[13] Swets J, Pickett R. Evaluation of Diagnostic Systems. Academic Press, 1982.

[14] Hanley J, McNeil B. The Meaning and Use of the Area under a Receiver Operating Characteristic (ROC) Curve. Radiology 1982;143:29–36.

[15] Bamber D. The area above the ordinal dominance graph and the area below the receiver operating characteristic graph. J Math Psychol 1975;12:387–415.

[16] Su J, Liu J. Linear Combinations of Multiple Diagnostic Markers. J Am Statist Assoc 1993;88(424):1350–1355.

[17] Kramar A, Faraggi D, Fortune A, B.Reiser. mROC: a computer program for combining tumour markers in predicting disease states. Computer Methods and Programs in Biomedicine 2001;66(2-3):199–207.

[18] Reiser B, Faraggi D. Confidence Intervals for the Generalized ROC Criterion. Biometrics 1997;53:644–652.

[19] Mee RW. Confidence Intervals for Probabilities and Tolerance Regions Based on a Generalization of the Mann-Whitney Statistic. J Am Statist Assoc 1990;85(441):793–800.

Address for correspondence:

Hans A. Kestler
Dept. of Neural Information Processing / University of Ulm
D-89069 Ulm / Germany
tel./fax: ++49-731-5002-4437/4156
hans.kestler@medizin.uni-ulm.de